Weather and Climate Extremes 20 (2018) 54–68

Contents lists available at ScienceDirect

Weather and Climate Extremes

journal homepage: www.elsevier.com/locate/wace

Australian climate extremes in the 21st century according to a regional climate model ensemble: Implications for health and agriculture

N. Herold [a,*], M. Ekström [b], J. Kala [c,a], J. Goldie [d,a], J.P. Evans [e]

[a] Climate Change Research Centre & ARC Centre of Excellence for Climate System Science, University of New South Wales, Sydney, Australia
[b] School of Earth and Ocean Sciences, Water Research Institute, Cardiff University, United Kingdom
[c] School of Veterinary and Life Sciences, Environmental and Conservation Sciences, Murdoch University, 6150, WA, Australia
[d] Fenner School of Environment & Society, Australian National University, Acton, ACT, Australia
[e] Climate Change Research Centre & ARC Centre of Excellence for Climate Extremes, University of New South Wales, Sydney, Australia

ARTICLE INFO

Keywords:
Australia
Climate extremes
Climate impacts
Health
Agriculture

ABSTRACT

The negative impacts of climate extremes on socioeconomic sectors in Australia makes understanding their behaviour under future climate change necessary for regional planning. Providing robust and actionable climate information at regional scales relies on the downscaling of global climate model data and its translation into impact-relevant information. The New South Wales/Australian Capital Territory Regional Climate Modelling (NARCliM) project contains downscaled climate data over all of Australia at a 50 km resolution, with ensembles of simulations for the recent past (1990–2009), near future (2020–2039) and far future (2060–2079). Here we calculate and examine sector-relevant indices of climate extremes recommended by the Expert Team on Sector-specific Climate Indices (ET-SCI). We demonstrate the utility of NARCliM and the ET-SCI indices in understanding how future changes in climate extremes could impact aspects of the health and agricultural sectors in Australia.

Consistent with previous climate projections, our results indicate that increases in heat and drought related extremes throughout the 21st century will occur. In the far future, maximum day time temperatures are projected to increase by up to 3.5 °C depending on season and location. The number of heatwaves and the duration of the most intense heatwaves will increase significantly in the near and far future, with greater increases in the north than south. All capital cities are projected to experience at least a tripling of heatwave days each year by the far future, compared to the recent past. Applying published heat-health relationships to projected changes in temperature shows that increases in mortality due to high temperatures for all cities examined would occur if projected future climates occurred today.

Drought and the number of days above 30 °C are also projected to increase over the major wheat-growing regions of the country, particularly during spring when sensitivity of wheat to heat stress is greatest. Assuming no adaptation or acclimatisation, published statistical relationships between drought and national wheat yield suggest that national yields will have a less than one quarter chance of exceeding the annual historical average under far future precipitation change (excluding impacts of future temperature change and CO_2 fertilization). The NARCliM data examined here, along with the ET-SCI indices calculated, provide a powerful and publicly available dataset for regional planning against future changes in climate extremes.

1. Introduction

Australia is exposed to a variety of climates due to its large size and meridional extent. Northern Australia is dominated by the seasonal migration of the Inter-tropical Convergence Zone (ITCZ) and the summer monsoon, leading to a mean annual precipitation of over 1,000 mm. Central and southern Australia are largely dominated by the subtropical high pressure belt, which is generally associated with clear skies, large sensible heat fluxes and is collocated with Australia's deserts. Conversely, the southern flank of the continent is influenced by wintertime mid-latitude cyclones, which bring substantial precipitation to southern portions of the mainland as well as the western half of Tasmania.

* Corresponding author.
E-mail address: nicholas.herold@unsw.edu.au (N. Herold).

https://doi.org/10.1016/j.wace.2018.01.001
Received 28 October 2017; Received in revised form 23 December 2017; Accepted 7 January 2018
Available online 5 April 2018

With such a wide range of climates, Australia also experiences a great diversity of climatic extremes, including heatwaves, floods, droughts and frosts (Westra et al., 2016). Understanding how extremes may change in the future is an important aspect of adaptation planning, as changes to rare but high impact climate events are likely to be a greater challenge to communities compared to changes in the average climate state. For example, while mean temperature in Alice Springs (Fig. 1) over the last half-century has increased from 20.4 to 21.2 °C, over the same period 35 more days each year now experience temperatures exceeding 35 °C. It is likely this latter fact has more serious implications for this community. Nonetheless, relatively small changes in the mean state can also cause climate extremes, such as during drought when persistently lower than normal (but not necessarily extremely low) precipitation leads to severe soil moisture shortages. Different extremes are also known to compound one another, such as the heatwaves that can follow the drying of soils during drought (Alexander, 2011).

Each 'extreme' causes a disruption to the natural and built environment. The nature of damage and the spatial and temporal footprint differs between each type of extreme (e.g. from sub-daily extreme precipitation that occurs locally to multi-year drought that can occur over a large region). Being exposed to a large number of different extremes, numerous socioeconomic sectors in Australia are at risk to adverse changes in their frequency, duration and intensity. For example, the "Millennium drought" (circa 1997–2010) significantly reduced national agricultural production and contributed to a reduction in the industry's GDP contribution from 2.9% to 2.4% (van Dijk et al., 2013). The 2009 Victorian heatwave led to 374 deaths (VGDHS, 2009), more than twice the number caused by the more highly publicised bushfires that it preceded (Teague et al., 2010). More generally, high temperatures throughout the country have been shown to increase morbidity (Bi et al., 2011) and mortality (Coates et al., 2014), as well as decrease labour productivity (Zander et al., 2015) and crop yields (Asseng et al., 2011). Given these diverse impacts there are substantial benefits to be gained from robust projections of climate extremes as well as the development and application of sector-specific climate indices with which to measure them.

Projections of climate extremes over Australia from global climate models have all indicated increases in hot extremes and decreases in cold extremes over the course of the 21st century. Alexander and Arblaster (2009, 2017) conducted comprehensive reviews of projected changes in climate extremes over Australia based on the third and fifth phases of the Coupled Modelling Intercomparison Project (CMIP3 and CMIP5, respectively; Meehl et al., 2007; Taylor et al., 2011). Based on the highest emission scenarios in CMIP5 these authors showed significant increases in all hot extremes for most locations in the future, as well as significant increases in dry days and significant decreases in annual precipitation over southwest Western Australia and the central east coast (Alexander and Arblaster, 2017). Results consistent with these have been found in other CMIP5 (Sillmann et al., 2013; Cowan et al., 2014) and CMIP3 analyses (Mpelasoka et al., 2008; Perkins and Pitman, 2009; Alexander and Arblaster, 2009; Kirono et al., 2011). Remarkably, CMIP5 data suggest that day time temperature extremes that currently occur every 20 years will occur every 5 or fewer years by the middle of the century (IPCC, 2012).

While General Circulation Models (GCM's) capture many aspects of large scale climate change well (IPCC, 2013), studies of changes in extremes and their impact on society require finer spatial resolutions and sometimes more processes (e.g. convective storms) than are available in GCMs. Dynamical and statistical downscaling have typically been used to bridge the resolution gap (Ekström et al., 2015). Existing high resolution dynamically downscaled projections over south-eastern Australia indicate that by 2020–2039 the frequency of heatwaves will significantly increase over most areas compared to 1990–2009, and by 2060–2079 the amplitude of the hottest heatwaves will also significantly increase (Argüeso et al., 2015). Conversely, mean heatwave temperatures may decrease in the future in some southeast Australian coastal regions due to a disproportionate increase in mild versus severe heatwaves (Argüeso et al., 2015). The same projections suggest that future changes in extreme

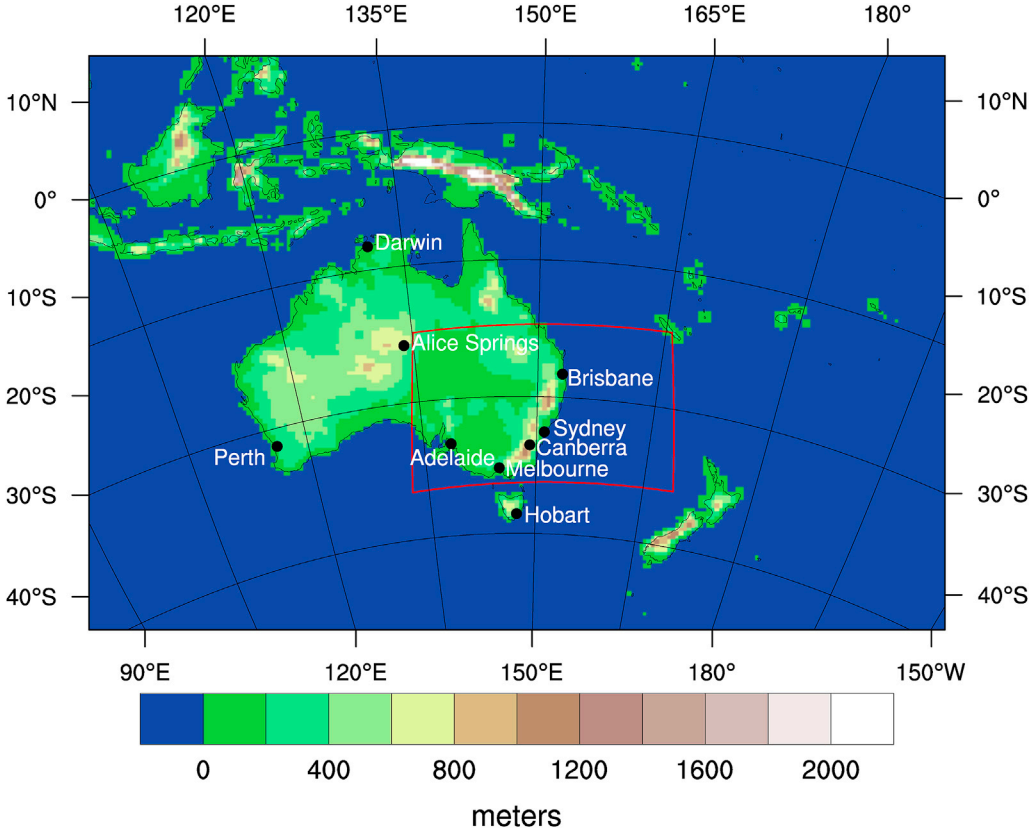

Fig. 1. The 50 km resolution model domain of the NARCliM project; the red box shows the outline of an inner finer resolution (10 km) domain. In the interest of estimating indices for continental Australia, only output from the 50 km resolution domain is used. See section two for details. Locations referenced in this study also shown.(For interpretation of the references to colour in this figure legend, the reader is referred to the Web version of this article.)

precipitation will be significant in far fewer locations compared to extreme temperature changes, although mean wet-day precipitation intensity will significantly increase over large parts of inland New South Wales (NSW) and Victoria (Evans et al., 2014a). Statistically downscaled CMIP5 projections over the NSW wheat belt also suggest an increased risk of heat-stress for crops and reduced risk of frost damage by the second half of the 21st century (Wang et al., 2016). In southwest Western Australia, dynamical downscaling indicates that mean and extreme daytime temperatures will increase more than night time temperatures, and that winter time precipitation will decrease (Andrys et al., 2017). These projections have highlighted substantial risks to Western Australia's viticulture (Firth et al., 2017).

Previous downscaling studies have been invaluable for providing projections of climate change over different regions of Australia. However, their relatively small spatial domains – typically chosen in favour of higher resolution – have precluded physically consistent projections of climate extremes across the continent. Here we use climate simulations from the NSW/Australian Capital Territory (ACT) Regional Climate Modelling project (NARCliM; Evans et al., 2014b) to examine projections of climate extremes over the whole of Australia during the 21st century. The NARCliM project is a joint initiative between the University of New South Wales and the New South Wales Office of Environment and Heritage to produce regional climate projections over NSW and the ACT as well as over all of Australia. To assess changes in climate extremes we calculate indices recommended by the Expert Team on Sector-specific Climate Indices (ET-SCI; Alexander et al. in revision). The ET-SCI is coordinated by the World Meteorological Organisation under the Commission for Climatology with a mandate to develop and promote climate extremes indices relevant to sectors (such as health, water and agriculture). These indices are calculated from daily values of minimum and maximum air temperature and precipitation. We note that other sector-relevant climate variables are not included in the calculation of these indices, such as humidity, which is important for understanding the physiological responses to heat stress (Monteith and Unsworth, 2013). Such exclusions are made because extremes indices frequently rely on long historical records (needed to account for long-term climate variability), which do not exist for more complex climate variables (Alexander et al. in revision). The NARCliM climate model data is available via the New South Wales Office of Environment and Heritage (OEH, 2017) and the ET-SCI indices calculated here are available upon request from the authors. For this study, we focus on indices relevant to the health and agriculture sectors, i.e. heatwaves, droughts and other temperature extremes, given the present sensitivity of these sectors to climate variability. Consequently, this paper does not represent a comprehensive assessment of sector-impacts from changing climate extremes, but is a demonstration of how the NARCliM data and ET-SCI indices may be used to improve our understanding of climate change impacts.

The remainder of this paper is organised as follows. In section two we describe the datasets used, including the NARCliM simulations and the ET-SCI indices. In section three we present projected changes in our selected climate extremes and in section four we review these projected changes in the context of known relationships with health and agriculture. We conclude the paper in section five. The supplementary material contains a catalogue of maps of future changes in all ET-SCI climate indices (see section 2.3).

2. Methods

2.1. NARCliM

The NARCliM project consists of regional climate simulations over two spatial domains, one covering the Australian and New Zealand land masses at 50 km spatial resolution and another covering NSW and the ACT at 10 km spatial resolution (Fig. 1; Evans et al., 2014b). These simulations were conducted with the Weather, Research and Forecasting model version 3.3 (Shamarock et al., 2008). Numerous studies describe various aspects of the 10 km (Evans et al., 2014a, 2016; Argüeso et al., 2015; Olson et al., 2016; Macadam et al., 2016) and 50 km domains (Clarke et al., 2016; Fita et al., 2016; Bao et al., 2017), although less work has been done on the 50 km domain, which is the exclusive focus of this study as it covers the entire continent. Three time periods were simulated in NARCliM; the recent past (1990–2009), near-future (2020–2039) and far-future (2060–2079). Each period consists of an ensemble of 12 simulations. Each ensemble member differs by its boundary and initial conditions as well as the physical parameterisations used in WRF. Four GCMs were used to provide boundary and initial conditions to the WRF simulations. These were chosen from CMIP3 by first removing unequivocally poor performing models over the Australian domain and then choosing models that spanned the plausible future change in temperature and precipitation found in the full ensemble, and that had the most independent errors. The GCMs chosen were MIROC3.2, ECHAM5, CCCM3.1 and the CSIRO-Mk3.0. Using data from these four GCMs, three different configurations of WRF were run (resulting in ensembles of 12). The WRF configurations included different combinations of parameterisations for the surface layer, planetary boundary layer, cumulus convection, short and long wave radiation and cloud microphysics. For the future periods, CMIP3 simulations forced by the Special Report on Emission Scenarios (SRES) A2 scenario were used. Current global CO_2 emissions data suggest we are following a trajectory slightly higher than SRES A2 (Peters et al., 2013), thus the projections presented here as they relate to temperature extremes may be conservative. For more details on the NARCliM experiment design see Evans et al. (2014b).

Because model output typically has a bias relative to the observed climate (given the error inherent in model boundary conditions, model design and our understanding of the climate system) a 'bias correction' was applied to the WRF output prior to calculating the ET-SCI indices (Evans and Argüeso, 2014). This correction is imposed to make the model simulation more similar to observed data in a distributional sense. There are concerns about this process (e.g. adverse impacts on inter-variable relationships and spatiotemporal relationships) as discussed by Ehret et al. (2012). However, for pragmatic reasons it is routinely applied to climate model output for use in impact work. Different methods for this correction exist, here it is an adjustment of the cumulative distribution functions of modelled daily maximum and minimum 2 m temperatures and total precipitation at each grid cell toward the observed cumulative distribution functions calculated from gridded observations (section 2.2). While this procedure adjusts modelled values toward observations it does not affect the sequence of modelled events (e.g. the number of consecutive dry or wet days) nor measures of exceedance of relative (i.e. percentile based) thresholds. Indeed, previous work has shown that this bias correction leads to significant improvements in indices that rely on absolute thresholds but not necessarily in indices based on percentiles (Gross et al., 2017). This bias correction has also been shown to improve simulated crop yields (Macadam et al., 2016). Bias correction was performed for all time periods using observations for 1990–2009, which assumes that biases in the future will be the same as in the recent past.

2.2. Observations

Substantial model evaluation has been performed on the output of the 10 km NSW/ACT domain (Evans et al., 2014a, 2016; Argüeso et al., 2015; Olson et al., 2016; Gross et al., 2017), however, the same has not been carried out for the 50 km Australian domain used here. In order to evaluate the WRF simulations we use daily minimum and maximum 2 m temperatures and daily precipitation from the Australian Water Availability Project (AWAP; Jones et al., 2009), the same dataset used to perform bias-correction. This dataset is available at a spatial resolution of 5 km and extends back to 1900. For our purpose the AWAP data was regridded to the WRF grid using inverse-distance weighting and was only considered from 1990 to 2009, corresponding to the simulations of the recent past. Given the bias correction applied to the WRF output, the biases in most of the calculated climate extremes indices are expectedly

Table 1
ET-SCI indices calculated in this study. Those in bold are examined in the main text, remaining are shown in supplementary material. TN = daily minimum temperature, TX = daily maximum temperature, TM = mean daily temperature = (TN + TX)/2, PR = daily precipitation total. *Heatwave aspects can be calculated for three definitions of heatwave: EHF (used in this study), TX90 and TN90 (See Perkins and Alexander, 2013 for details).

Name	Definition	Units
FD	Number of days when TN < 0 °C	days
TNlt2	**Number of days when TN < 2 °C**	**days**
TNltm2	Number of days when TN < −2 °C	days
TNltm20	Number of days when TN < −20 °C	days
ID	Number of days when TX < 0 °C	days
SU	Number of days when TX > 25 °C	days
TR	Number of days when TN > 20 °C	days
GSL	Annual number of days between the first occurrence of 6 consecutive days with TM > 5 °C and the first occurrence of 6 consecutive days with TM < 5 °C	days
TXx	**Warmest daily TX**	**°C**
TNn	Coldest daily TN	°C
WSDI	Annual number of days contributing to events where 6 or more consecutive days experience TX > 90th percentile	days
WSDId	Annual number of days contributing to events where *d* or more consecutive days experience TX > 90th percentile	days
CSDI	Annual number of days contributing to events where 6 or more consecutive days experience TN < 10th percentile	days
CSDId	Annual number of days contributing to events where *d* or more consecutive days experience TN < 10th percentile	days
TXgt50p	Percentage of days where TX > 50th percentile	%
TX95t	Value of 95th percentile of TX	°C
TMge5	Number of days when TM > = 5 °C	days
TMlt5	Number of days when TM < 5 °C	days
TMge10	Number of days when TM > = 10 °C	days
TMlt10	Number of days when TM < 10 °C	days
TXge30	**Number of days when TX > = 30 °C**	**days**
TXge35	Number of days when TX > = 35 °C	days
TXdTNd	Annual count of *d* consecutive days where both TX > 95th percentile and TN > 95th percentile, where 10 > = *d* >= 2	events
HDDheatn	Annual sum of *n* - TM (where *n* is a user-defined location-specific base temperature and TM < *n*)	degree-days
CDDcoldn	Annual sum of TM - *n* (where *n* is a user-defined location-specific base temperature and TM > *n*)	degree-days
GDDgrown	Annual sum of TM - *n* (where *n* is a user-defined location-specific base temperature and TM > *n*)	degree-days
CDD	Maximum number of consecutive dry days (when PR < 1.0 mm)	days
R20 mm	Number of days when PR > = 20 mm	days
PRCPTOT	Sum of daily PR > = 1.0 mm	mm
R95pTOT	100*r95p/PRCPTOT	%
R99pTOT	100*r99p/PRCPTOT	%
RXdday	Maximum *d*-day PR total	mm
SPI	Measure of drought using the Standardised Precipitation Index. See McKee et al. (1993) and the WMO SPI User guide (WMO, 2012) for details.	unitless
SPEI	**Measure of drought using the Standardised Precipitation Evapotranspiration Index. See Vicente-Serrano et al. (2010) for details.**	**unitless**
HWN*	**Heatwave Number: The number of individual heatwaves that occur each summer (Nov – Mar in southern hemisphere and May – Sep in northern hemisphere). For EHF heatwaves are counted over the entire year. A heatwave is defined as 3 or more days where either the EHF is positive, TX > 90th percentile or where TN > 90th percentile, depending on the definition of heatwave chosen*. Percentiles are calculated from the recent past simulation (1990–2009).**	**unitless**
HWF*	**Heatwave Frequency: The number of days that contribute to heatwaves identified by HWN.**	**days**
HWD*	**Heatwave Duration: The length of the longest heatwave identified by HWN.**	**days**
HWM*	**Heatwave Magnitude: The mean temperature of all heatwaves identified by HWN.**	**°C (°C^2 for EHF)**
HWA*	**Heatwave Amplitude: The peak daily value in the hottest heatwave (defined as the heatwave with highest HWM).**	**°C (°C2 for EHF)**
CWN	Coldwave Number: The number of individual "coldwaves" that occur each year as defined by the Excess Cold Factor (Nairn and Fawcett, 2013).	unitless
CWF	Coldwave Frequency: The number of days that contribute to coldwaves as identified by CWN.	days
CWD	Coldwave Duration: The length of the longest coldwave identified by CWN.	days
CWM	Coldwave Magnitude: The mean temperature of all coldwaves identified by CWN.	°C^2
CWA	Coldwave Amplitude: The minimum daily value in the coldest coldwave (defined as the coldwave with lowest CWM).	°C^2
TXbdTNbd	Annual number of *d* consecutive days where both TX < 5th percentile and TN < 5th percentile, where 10 > = *d* >=2	events
DTR	Mean difference between daily TX and daily TN	°C
TNx	Warmest daily TN	°C
TXn	Coldest daily TX	°C
TMm	Mean daily mean temperature	°C
TXm	Mean daily maximum temperature	°C
TNm	Mean daily minimum temperature	°C
TX10p	Percentage of days when TX < 10th percentile	%
TX90p	Percentage of days when TX > 90th percentile	%
TN10p	Percentage of days when TN < 10th percentile	%
TN90p	Percentage of days when TN > 90th percentile	%
CWD	Maximum annual number of consecutive wet days (when PR > = 1.0 mm)	days
R10 mm	Number of days when PR > = 10 mm	days
Rnnmm	Number of days when PR > = *nn*	days
SDII	Annual total PR divided by the number of wet days (when total PR > = 1.0 mm)	mm/day
R95p	Annual sum of daily PR > 95th percentile	mm
R99p	Annual sum of daily PR > 99th percentile	mm
Rx1day	Maximum 1-day PR total	mm
Rx5day	Maximum 5-day PR total	mm

small, with the exceptions of indices involving counts of wet or dry days, such as Consecutive Wet Days and Consecutive Dry Days (Supplementary Fig. 12 and 13). See the supplementary material for a comparison of the extremes indices analysed in this paper with indices calculated from the AWAP data.

2.3. Climate extremes indices

Table 1 lists the ET-SCI indices calculated from the NARCliM climate model ensemble. This was performed with the ClimPACT software developed under the auspices of the ET-SCI (Alexander et al. in revision). As previously mentioned, we focus on indices relevant to the health and agricultural sectors. Specifically, we examine heatwaves defined by the Excess Heat Factor (EHF), drought defined by the Standardised Precipitation-Evapotranspiration Index (SPEI), as well as several simple temperature indices including TXx, TXm, TXge35, TXge30 and TNlt2 (Table 1 for definitions).

Multi-model means of all three time periods are shown in maps while the inter-model spread for specific locations or regions are shown in box plots. Maps of all ET-SCI indices are available in the supplementary material. Where applicable, we calculate seasonal values corresponding to Summer (DJF: December-January-February), Autumn (MAM: March-April-May), Winter (JJA: June-July-August) and Spring (SON: September-October-November). We note that three-month seasons are not representative of all climatic regimes, such as for tropical Australian rainfall, but are useful at subtropical and mid-latitudes where the majority of the population live. For all indices that rely upon a base period for calculation we use the recent past (i.e. 1990–2009). Details of the heatwave, drought and other indices used in this study are given below.

There are numerous definitions of heatwaves, many of which are region or discipline dependant (Perkins and Alexander, 2013). Here we define heatwaves using the EHF (Nairn and Fawcett, 2013), the index used for forecasting heatwaves by the Australian Bureau of Meteorology. The EHF has been shown to more highly correlate with heat-related deaths than daily mean or maximum temperature alone and thus is a better indicator of health impacts (PwC, 2011; Nairn and Fawcett, 2013; Scalley et al., 2015). To assess the various aspects of heatwaves we use the framework recommended by Perkins and Alexander (2013) which includes five definition-independent 'heatwave aspects' that are described in Table 1. These are heatwave number (the number of heatwave events), heatwave frequency (the number of days contributing to heatwaves), heatwave duration (the length of the most intense heatwave), heatwave magnitude (the mean intensity of all heatwaves) and the heatwave amplitude (the intensity of the hottest day of the hottest heatwave). These heatwave aspects are by definition calculated annually.

The EHF combines a comparison of daily temperatures to climatology, with a comparison of daily temperatures to the preceding 30 days (thus explicitly considering acclimatisation). These two measures are represented by excess heat indices (EHI) of significance (sig) and acclimatisation (acc), respectively.

$$EHI_{sig} = (T_i + T_{i-1} + T_{i-2})/3 - T_{95} \quad (1)$$

$$EHI_{acc} = (T_i + T_{i-1} + T_{i-2})/3 - (T_{i-3} + \ldots + T_{i-32})/30 \quad (2)$$

Where T_i represents the mean daily temperature, $(TX_i + TN_i)/2$, of day i and T_{95} represents the 95th percentile of all daily mean temperatures over the base period 1990–2009 (Nairn and Fawcett specify 1961–1990 as the base period, however, this is adjusted given the NARCliM experimental design). The use of mean temperature as opposed to maximum (i.e. daytime) temperature permits this index to account for the accumulation of heat that may occur due to high night time temperatures, which can be critical in determining the severity of a heatwave (e.g. Karl and Knight, 1997). Calculating T_{95} over all calendar days results in most heatwave days being identified during summer months, and while heatwaves can occur at any time of year (Perkins and Alexander, 2013), deaths due to heatwaves in Australia overwhelmingly occur during summer (Coates et al., 2014).

The EHF is then a combination of the above two excess heat indices.

$$EHF = EHI_{sig} \times \max(1, EHI_{acc}) \quad (3)$$

The EHF has units of $°C^2$. While this unit is more difficult to interpret than temperature, the quadratic relationship between EHI_{sig} and EHI_{acc} is consistent with observed relationships between heat events and sectoral responses (Nairn and Fawcett, 2013). Consistent with Perkins and Alexander (2013), to identify heatwave events we require that the EHF be positive for a minimum of three consecutive days.

While the EHF is a more advanced metric for gauging heat-health impacts, it has only been developed recently and there are few case studies using it currently (Langlois et al., 2013; Nairn and Fawcett, 2013; Jegasothy et al., 2017). Conversely, numerous studies have examined the relationship between health and more simple temperature thresholds. Specifically, TXm, TXge35 and TXge30 have been used in previous studies to quantify the relationship between heat and health and thus we apply these relationships to future projections of the indices (section 4.1).

Wheat is the largest contributor to Australia's agricultural sector (Hughes et al., 2015) and is vulnerable to temperature extremes and drought. Temperatures above 30 °C for a single day have been shown to significantly reduce wheat grain development (Saini and Aspinall, 1982), while freezing temperatures also damage crops (Marcellos and Single, 1975). Thus we use TXge30 and TNlt2 to quantify the effects of heat stress and frost damage on crops. The choice of TNlt2 is based on evidence that air temperatures in the canopy can be notably higher than those at the surface of a crop (Marcellos and Single, 1975; Kala et al., 2009), thus we measure 'frost risk days' as the number of days where night time temperature is below 2 °C (TNlt2).

Like heatwaves, droughts are complex and lack a unified definition. Despite this, all definitions highlight a deficit of soil-moisture caused at least by insufficient precipitation. In this study we use the SPEI to quantify drought (Vicente-Serrano et al., 2010), which is a modified form of the Standardised Precipitation Index (SPI; McKee et al., 1993). The SPI is a popular index due to its simplicity, flexibility and minimal data requirements (only monthly precipitation is required) and is the drought index recommended by the World Meteorological Organisation (WMO, 2012). The SPI measures drought by comparing standardised accumulations of precipitation each month and for a user-specified number of preceding months to equivalent calendar months within a base period, after fitting the latter to a Gamma distribution. The ability to specify the number of preceding months gives the SPI the ability to monitor droughts over different time scales. For example, hydrological droughts associated with groundwater and streamflow may occur on time scales of 24–48 months, whereas meteorological droughts may occur after one month of insufficient precipitation. Despite these benefits, a limitation of the SPI is that it does not consider the effect of evapotranspiration on the surface water balance. The SPEI addresses this by explicitly subtracting potential evapotranspiration from precipitation accumulations and has been shown to more accurately capture changing drought intensity under global warming (Vicente-Serrano et al., 2010). Here we use the Hargreaves method to calculate evapotranspiration (see Supplementary section 1 for details), consistent with previous work (Herold et al., 2016). Furthermore, we use the 3-month SPEI, a typical time scale for soil moisture drought and thus of agricultural relevance. SPEI values are

Table 2
SPEI/SPI drought categories (WMO, 2012).

SPEI/SPI	Drought severity
2.0 and higher	Extremely wet
1.5 to 1.99	Very wet
1.0 to 1.49	Moderately wet
−0.99 to 0.99	Near normal
−1.0 to −1.49	Moderately dry
−1.5 to −1.99	Severely dry
−2 and lower	Extremely dry

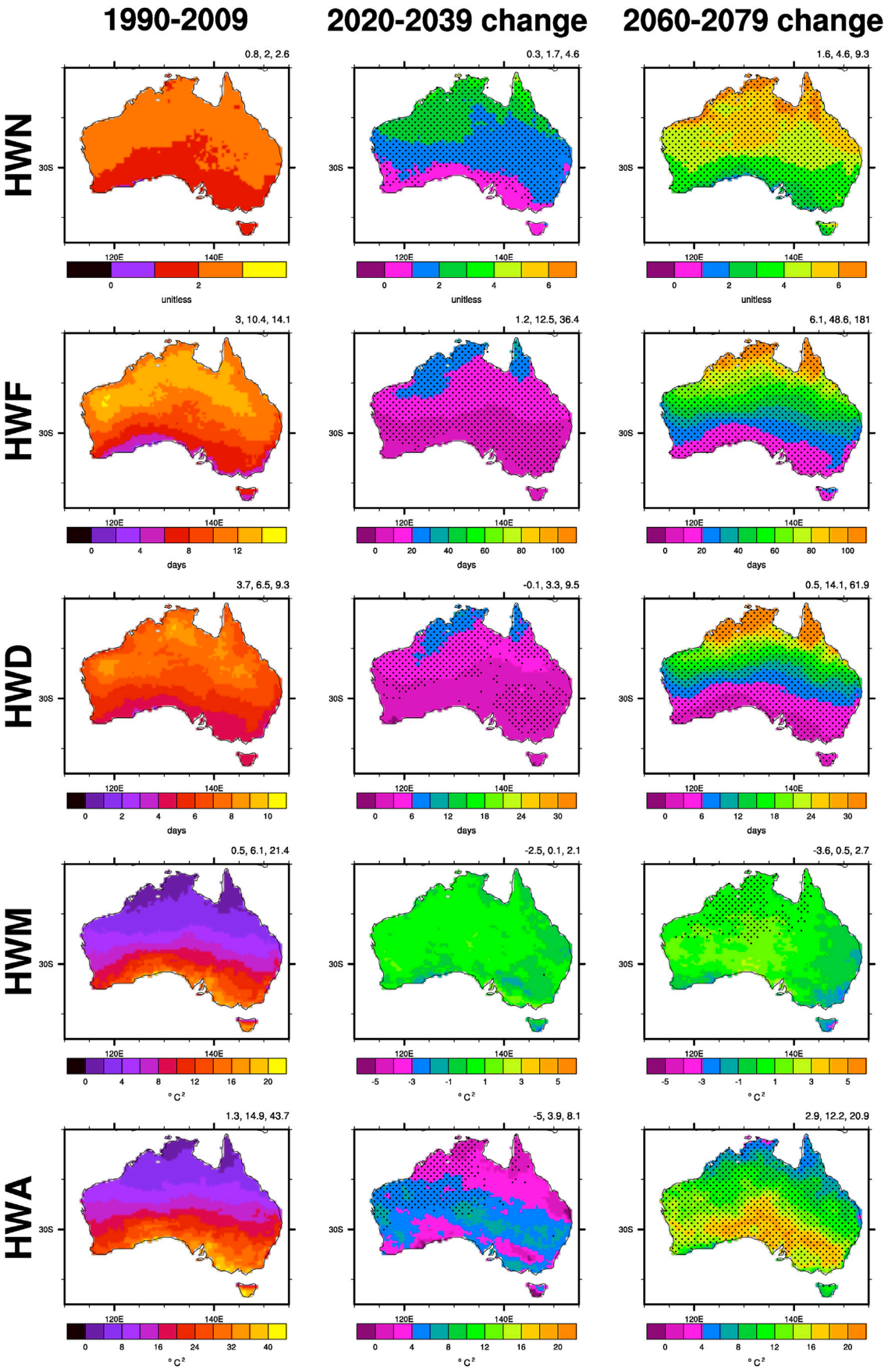

continued on next page

calculated monthly and in this instance the SPEI value for month *i* (e.g. May) represents a comparison of precipitation minus potential evapotranspiration accumulations over months *i-2, i-1* and *i* (e.g. March, April, May) to the equivalent three month accumulations over a base period (in this case 1990–2009). Given the SPEI is standardised, positive values represent wetter-than-average conditions while negative values represent drier-than-average conditions. See Table 2 for a common interpretation of SPEI severity.

2.4. Significance

To take advantage of the large ensemble size in NARCliM we utilise the convention of Tebaldi et al. (2011) to identify regions of statistically significant change when mapping our results. This method considers the presence of internal climate variability and assesses the degree of consensus between models on the significance of a change. For each grid cell, when 50% or more of the model ensemble (of which there are 12 members) show significant change based on a *t*-test where $p = .05$, and at least 80% of those models agree on the direction of change, we display the multi-model mean in colour and with stippling. This indicates a significant increase or decrease in the corresponding climate index. If at least 50% of the model ensemble shows significant change but less than 80% of those models agree on the direction of change, we do not show the multi-model mean but instead colour the grid cell white. This indicates significant model disagreement on the projected change. Lastly, if less than 50% of the model ensembles show a significant change we show the multi-model mean in colour with no stippling. This indicates that the projected multi-model mean change is within the variability of the simulated present day climate in most models.

3. Projections

3.1. Heatwaves

Fig. 2 shows the five heatwave aspects assessed in this study (by row), for the recent past (left column) and for changes in the near and far future (middle and right columns, respectively). In the near future the number of heatwaves double in the country's north, with three events annually in the recent past and an additional three to four occurring in the near future (Fig. 2 first row). In the far future heatwaves triple along the continent's northern fringe, increasing by six or more compared to the recent past. In the south increases are smaller, with two heatwaves per year in the recent past and an increase of one to two in the near future and three to four in the far future.

Change in heatwave frequency (the number of days contributing to heatwaves) expectedly follows a similar pattern to changes in heatwave number (Fig. 2 second row). The number of heatwave days in the north doubles in the near future, compared to the recent past, and is over six times higher in many northern regions in the far future. This is attributed to the smaller temperature variability of the tropics and thus the relatively small increases in temperature needed to exceed the 95th percentile on which the EHF is based (section 2.3). Changes in heatwave days are substantially smaller in the south but still increase by a factor of two to three by the far future.

The most extreme heatwaves in the recent past were approximately six to nine days long in the central and northern parts of the country, and three to six days long in the south (Fig. 2 third row). In the near future the most extreme heatwaves will approximately double in length in the north and by the far future will be over one month long.

There is some evidence that ocean thermal inertia and the Great Dividing Range (along the east coast of Australia, Fig. 1) moderate increases in heatwave frequency and duration along Australia's coasts, notably reducing changes there compared to those that occur inland (Fig. 2 second row). Interestingly, for heatwave frequency, number and duration the northern half of Tasmania responds more strongly to far future climate change than does the south-eastern fringe of the mainland (Fig. 2).

Heatwave magnitude does not change significantly over most of the continent in the future and decreases in some regions in the east (Fig. 2 fourth row). This has been reported by Argüeso et al. (2015) in southeast Australia and attributed to a disproportionate increase in mild versus strong heatwaves that consequently lowered mean heatwave intensity. We note a similar behaviour in the change in coldwave temperatures, where coldwaves are defined inversely to EHF (Nairn and Fawcett, 2013). On average, coldwaves in many parts of the country get colder into the far future despite increases in mean temperature, a side-effect of a reduction in the number of relatively mild coldwaves (Supplementary Fig. 1). Changes in heatwave number (HWN), frequency (HWF) and duration (HWD) are larger in the north than south in both future periods, while heatwave amplitude (HWA) increases more in the south.

A comparison of capital cities (Fig. 1) highlights the difference in heatwave frequency between the major population centres, for Darwin particularly, which exhibits an ensemble median of 37 and 135 heatwave days each year in the near and far future, respectively, up from only 11 days in the recent past (Fig. 3a). Thus, in the far future over four months of the year will exhibit heatwave conditions in Darwin, almost all of which will occur during November to March. However, the model ensemble also exhibits the largest spread for Darwin, from less than 100 heatwave days a year to over 200 days. Melbourne, Adelaide and Hobart will experience the smallest increases in heatwave days, though by the far future period this will still constitute an at least tripling compared to the recent past. In contrast to its large changes in heatwave frequency, Darwin experiences the smallest increases in heatwave amplitude in the future, commensurate with its low temperature variability (Fig. 3b). Cities south of Brisbane exhibit similar changes in heatwave amplitude, with Adelaide experiencing the largest increase in the far future.

3.2. Daytime temperature extremes

Changes in maximum daytime temperature, TXx, indicate how the rightmost tail of the probability distribution will change in the future. Seasonal values of TXx are shown in Fig. 4. Increases in the near future are significant over most of the continent in all seasons and by the far future are significant over the entire continent in all seasons. The largest increases in the near future occur on the west coast during winter and in the far southeast during spring, whereas the smallest increases occur in the southeast during winter and autumn. In the far future an east-west gradient is apparent in all seasons, with the largest increases occurring in the west.

The number of days where daytime temperature exceeds 30 °C, TXge30, represents a threshold index that in most locations and seasons is less extreme than TXx. It has also been linked to heat-related mortality (see section 4.1). In the near future during spring and summer, areas that do not currently experience temperatures over 30 °C on all days of the season (i.e. central and southern Australia) will experience significant increases (Fig. 5 middle column). The largest increase in days above 30 °C will be in autumn and winter in the north in both the near and far future. By the far future in autumn, winter and spring, there will be on average more than one extra week of days above 30 °C across the country compared to the recent past.

Fig. 2. Multi-model means of fives heatwave aspects (Table 1 for definitions) calculated for the Excess Heat Factor (EHF; section 2.3). Left column: recent past, middle column: near-future change from recent past, right column: far-future change from recent past. Top row: heatwave number (HWN), second row: heatwave frequency (HWF), third row: heatwave duration (HWD), fourth row: heatwave magnitude (HWM), bottom row: heatwave amplitude (HWA). Stippling indicates significant change (section 2.4 for method). Values at the top right of each panel represent the minimum, mean and maximum of the plotted field.

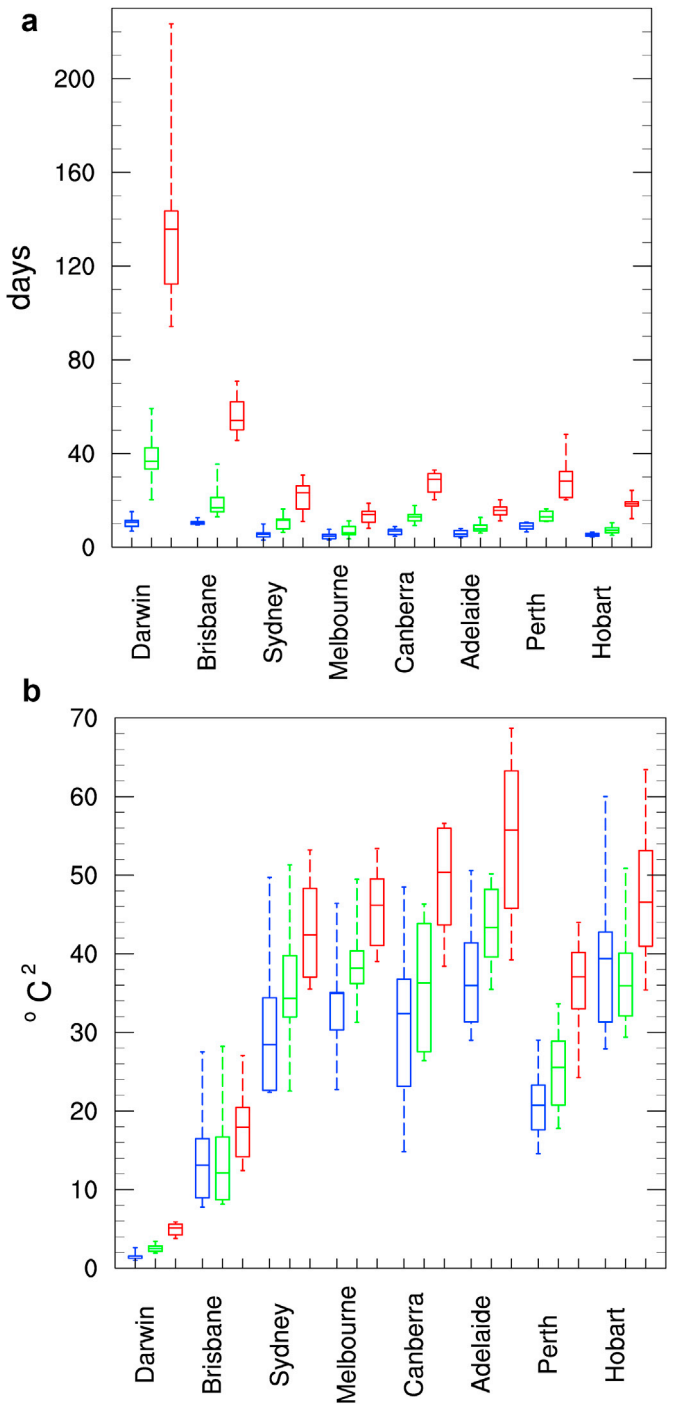

Fig. 3. Box and whisker plots for a) heatwave frequency (HWF) and, b) heatwave amplitude (HWA) at each city for the recent past (blue), near-future (green) and far-future (red). Bottom and top of boxes indicate the 25th and 75th percentiles, respectively. Middle line is the ensemble median and whiskers extend to the lowest and highest ensemble member. Data is taken from the closest grid cell to each city.

3.3. Drought

We measure drought intensity for all four seasons using the 3-month SPEI for the last month of each season (e.g. drought intensity for December-January-February is represented by the 3-month SPEI value for February). All SPEI values have been calculated using the recent past (1990–2009) as the base period. Since the SPEI is standardised values in the base period are by definition close to zero and thus not shown. In other words, Fig. 6 should be interpreted as the change in drought conditions relative to the recent past. In the near future, almost all regions of the continent exhibit similar soil moisture conditions compared to the recent past, with the exception of some significant drying in the southwest and southeast during spring (Fig. 6 top row). In the far future drought substantially intensifies in spring to cover a large portion of the southern half of the continent (Fig. 6 bottom row), with moderate and severe drought in the southwest and moderate drought in the southeast (Table 2 for SPEI severity). For comparison, severe to extreme drought conditions occurred in Sydney seven times during the period of the Millennium drought (circa 1997–2010). The southwest and southeast of the continent also coincide with areas of large increases in spring TXx (Fig. 4). Less intense (but still significant) drying occurs in the southwest during winter and summer, and some significant drying and model disagreement occurs in the north during winter.

3.4. Hot days and frost nights in wheat growing regions

Here we separate the wheat growing areas of Australia into three regions and show changes in the spatial mean of TXge30 and TNlt2 for each (see inset of Fig. 7a for regions). While regional means can neglect a considerable degree of spatial heterogeneity (Zheng et al., 2012) and different wheat varieties are grown in different regions we treat these values as indicative of the changes that may influence future sowing and harvesting periods. More spatial detail can be gained from the corresponding seasonal maps of TXge30 and TNlt2 (Supplementary Figs. 41 and 32, respectively).

Given the southerly locations of the wheat growing regions none currently experience day time temperatures over 30 °C during June, July or August (Fig. 7a). Future increases in TXge30 are large in middle to late spring, the flowering period for wheat, with little or no increases during winter in all three regions. The western and eastern regions experience substantially larger increases in spring and summer hot days compared to the southern region.

The western wheat growing region experiences relatively few frost risk days and by the far future will likely experience less than two on average each month during winter (Fig. 7b). The eastern region experienced the most frost in the recent past but by the far-future the number of frost risk days in August will be the same as what occurred in September in the recent past, and the number of frost risk days that occur in September will be similar to what occurred in October in the recent past. More dramatically, the most frost risk days of any month in the far future will likely be less than what occurred any time in winter in the recent past, in all three regions.

4. Discussion

4.1. Linking changes in climate extremes to health impacts

Increasing temperatures can lead to increases in excess mortality (the number of deaths above that expected) as well as increases in the transmission of vector borne diseases. We combine our results with several studies that have measured the relationship between temperature and daily excess mortality in several Australian cities (Guest et al., 1999; Hu et al., 2008; Bi et al., 2008; Williams et al., 2012a, b), and between temperature and increases in cases of the Ross River Virus near Hobart (Werner et al., 2012). These studies used indices equivalent to ET-SCI indices described in Table 1 and thus can be applied to our results to provide simple estimates of the health impacts of future climate change, as summarised in Table 3. However, the literature on heat-health relationships in Australia is more extensive than reflected in these analyses, see for example Oppermann et al. (2017) for a review on heat-health relationships in a tropical Australian setting, and Hanna et al. (2010) for impacts on working Australians.

Hu et al. (2008) found that in Sydney during summer, mortality increases by 0.9% for each °C increase in mean daytime temperature. Based

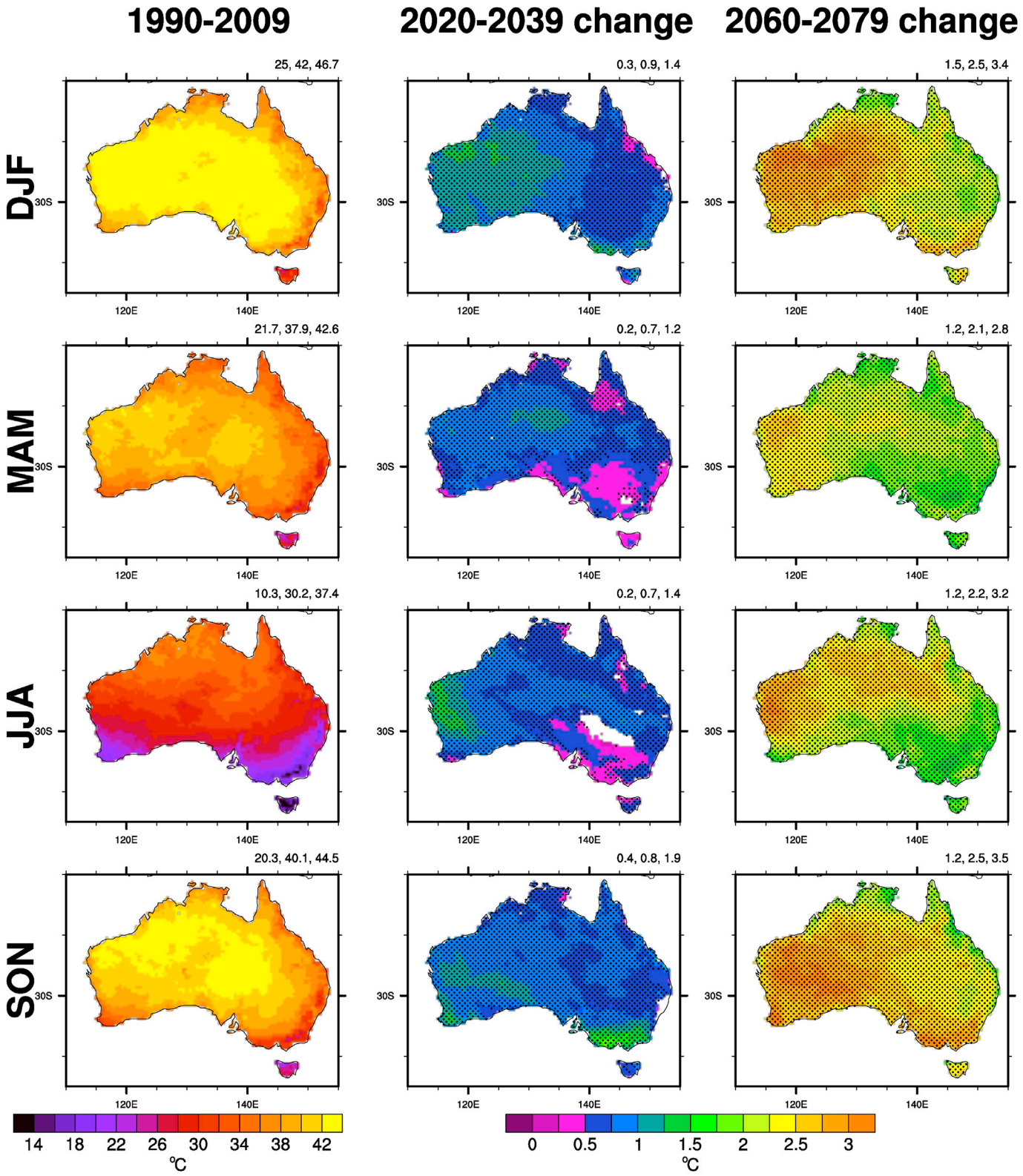

Fig. 4. Multi-model means of TXx (maximum daytime temperature) for each time period and season. Left column: recent past, middle column: near-future change from recent past, right column: far-future change from recent past. Top row: DJF, second row: MAM, third row: JJA, bottom row: SON. Stippling indicates significant change (section 2.4 for method). Values at the top right of each panel represent the minimum, mean and maximum of the plotted field.

on this relationship and projected increases in summer TXm (Table 1 for definition) there would be a 0.9% and 1.8% increase in annual all-age mortality due to increased summer daytime temperatures under a near and far future climate, respectively (Table 3). In Brisbane, mortality for people aged 65 years and older has been found to increase by 7% per °C increase in mean summer daytime temperatures (Bi et al., 2008). Based on this relationship and projected increases in summer TXm there would be a 3.5% and 11.9% increase in mortality for this age group under a near

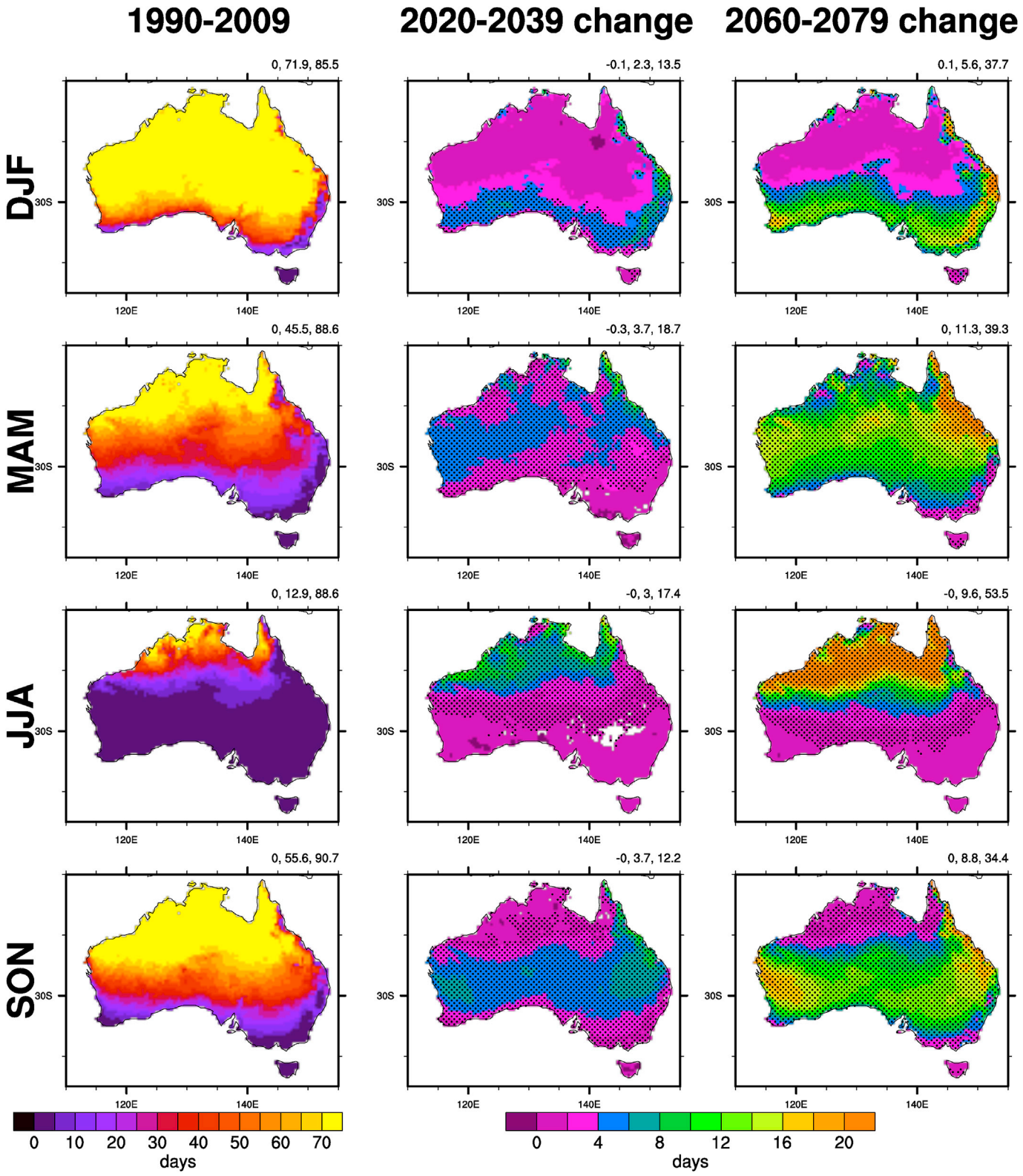

Fig. 5. Same as Fig. 4 except for TXge30 (number of days with daytime temperatures at or above 30 °C).

and far future climate, respectively. Guest et al. (1999) quantified excess mortality for multiple temperature thresholds in most major cities which allows us to estimate the number of heat-related deaths that would occur under near and far future climates (Table 3). Estimated increases in daily excess mortality due to daytime temperatures above 30 °C are highest for Sydney and Brisbane under a far future climate (76.8 and 32.5 more deaths, respectively). For Sydney this is largely a result of the population's sensitivity to high temperatures, whereas for Brisbane it is largely due to the increase in the number of hot days. Williams et al. (2012a) showed that excess mortality in Adelaide across all age groups increases when warm season daytime temperatures exceed 30 °C. Days at or exceeding 30 °C in Adelaide are set to increase from 55 in the recent

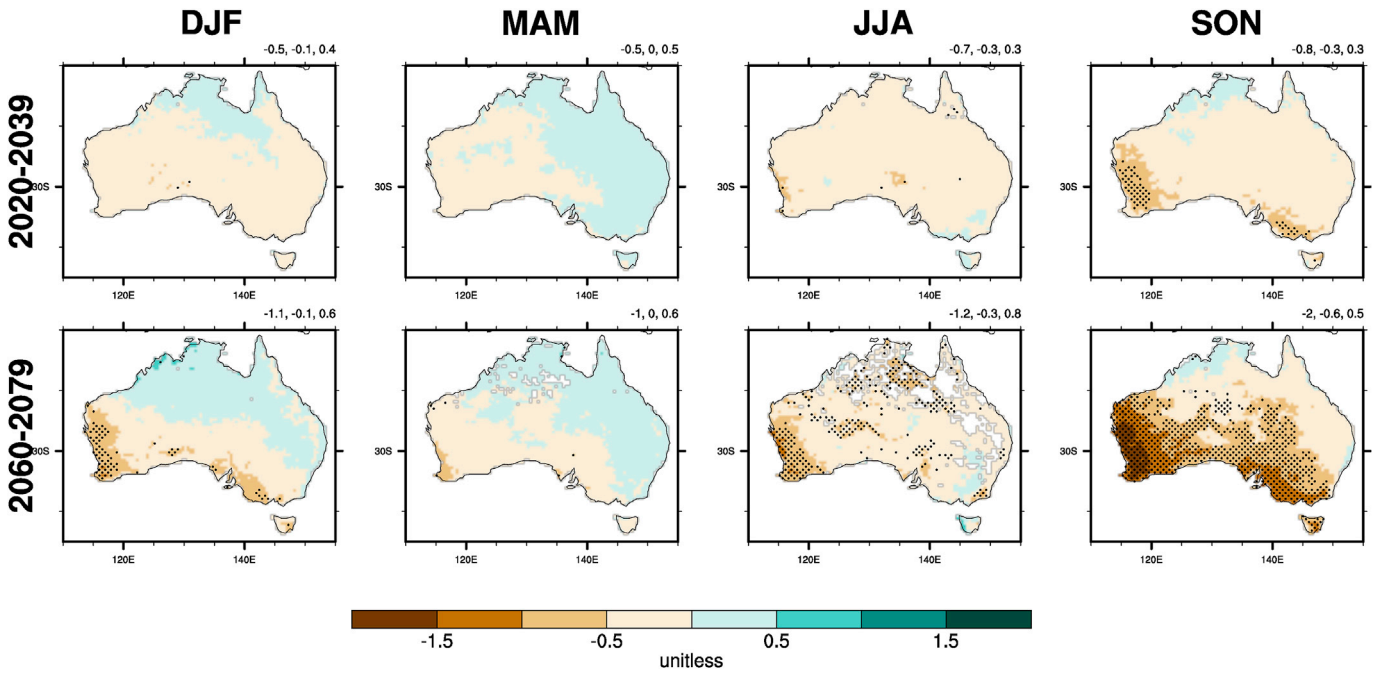

Fig. 6. Multi-model means of the Standardised Precipitation-Evapotranspiration Index (SPEI; section 2.3) for each season. Top row: near-future, bottom row: far-future. First column: DJF, second column: MAM, third column: JJA, fourth column: SON. A base period of 1990–2009 (i.e. the recent past) is used to calculate SPEI for all time periods. Thus, by definition the SPEI is close to zero during the recent past and excluded here. Future values should be interpreted as increases or decreases in drought conditions relative to the recent past. See Table 2 for an interpretation of drought intensity. Stippling indicates significant change (section 2.4 for method). Values at the top right of each panel represent the minimum, mean and maximum of the plotted field.

past to 60 in the near future and to 75 in the far future. Similarly, Perth experiences all age excess mortality increases when warm season daytime temperatures exceed 34–36 °C (Williams et al., 2012b). Days at or above 35 °C are set to increase from 20 in the recent past to 25 in the near future and to 40 in the far future. The EHF has also been shown to correlate well with heat-related deaths (PwC, 2011; Langlois et al., 2013) and demonstrates potential to anticipate the timing of health impacts from heatwaves. Indeed, excess mortality due to EHF heatwaves has been calculated for several Australian cities (PwC, 2011), though data availability prevents the same methodology being applied here.

While Australia experiences relatively low incidences of vector borne diseases it has been shown, for example, that cases of the Ross River virus increase by 23.9% per °C increase in monthly mean daytime temperature near Hobart (Werner et al., 2012). NARCliM projections indicate that TXm in Hobart will increase in April – when infections are most likely – by 0.6 °C in the near future and by 1.9 °C in the far future, equivalent to increases in infections of 14% and 45%, respectively, if these climates occurred today (Table 3).

We emphasize that these health impacts only consider the effect of future climate change on the current population, and thus changes in demographics, population size and distribution, the probability distribution of daily temperature, air pollution, acclimatisation and other environmental factors are not taken into account. Population growth would likely increase estimates of absolute excess mortality, though factors such as acclimatisation and the increased availability of air-conditioning, for example, would likely decrease them. However, reductions due to acclimatisation are a source of considerable uncertainty (Gosling et al., 2017) and there are physiological (e.g. Sherwood and Huber, 2010) and behavioural limits (e.g. 100% penetration of air-conditioning) to adaptation. Furthermore, EHF already captures some aspect of physiological acclimatisation. Nonetheless, these estimated health impacts should be interpreted as the hypothetical effect of future climates occurring in the present.

More sophisticated heat-health relationships have also been examined in the literature, which relate climate variables such as minimum daily temperature, humidity, temperature across days and/or percentile thresholds (e.g. Loughnan et al., 2010a; Tong et al., 2010; Pearce et al., 2016) to a variety of health impacts such as ambulance call-outs and emergency department presentations, along with more demographically or medically stratified analyses (e.g. Hansen et al., 2008a, b; Tong et al., 2010; Williams et al., 2012a, b; Turner et al., 2013). High temperatures also have health impacts beyond mortality, including increased morbidity (e.g. Naish et al., 2009; Loughnan et al., 2010b; Bi et al., 2011), decreased labour productivity (Zander et al., 2015) and the cessation of vital community services (Hughes and Steffen, 2014). However, accounting for future changes in non-climatic factors when estimating health impacts, as well as considering a larger array of health outcomes and climatic variables, involves large uncertainties across multiple disciplines (e.g. Huang et al., 2011) and is beyond the scope of this study.

4.2. *Linking changes in climate extremes to agricultural impacts*

The most direct way climate change impacts agriculture is via modifications to the timing and/or intensity of temperature and precipitation (e.g. Nicholls, 1997; Crimp et al., 2016; Madadgar et al., 2017). In the far future spring soil moisture is set to decrease significantly across southern Australia while winter and summer soil moisture will decrease in the southwest (Fig. 6). The combination of more frequent hot days (Fig. 7a) and significantly decreased soil moisture during the spring growing season will impose a permanent burden on rain-fed crops in the southwest and southeast, a finding consistent with previous regional climate modelling (Andrys et al., 2017; Firth et al., 2017). Increases in daytime temperature extremes in the southwest are also projected to be among the highest in the country during spring (Fig. 4), a time when wheat is most vulnerable to heat stress.

Decreases in frost risk days – particularly in the southern and eastern wheat growing regions – should allow sowing and harvesting to move forward to take advantage of warmer winters and avoid hotter springs. We note, however, that frost occurrences have increased over recent

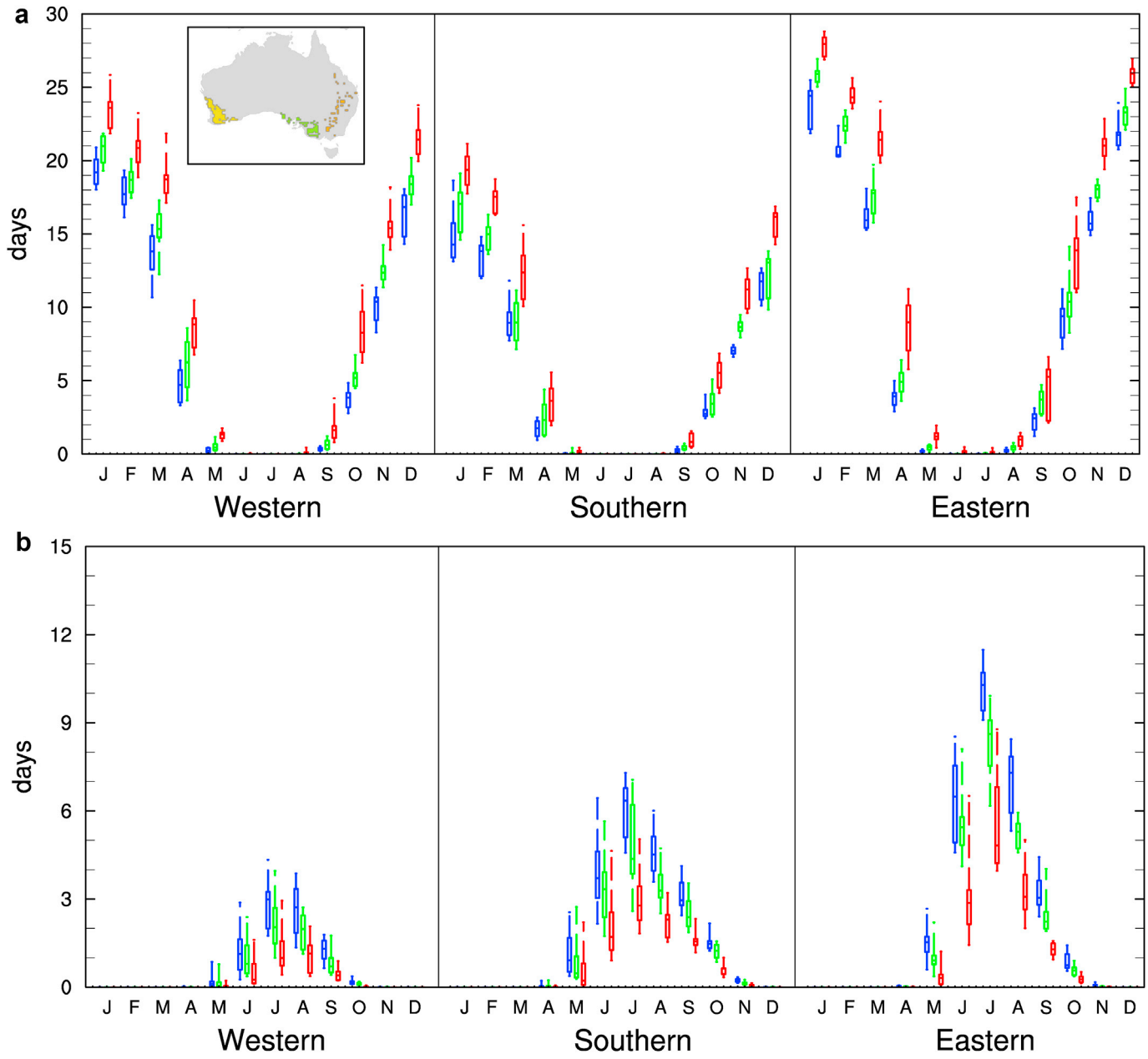

Fig. 7. Box and whisker plots showing spatial means of a) TXge30 (number of days with daytime temperatures at or above 30 °C) and, b) TNlt2 (number of days with night time temperatures below 2 °C) over the western, southern and eastern wheat growing regions for the recent past (blue), near-future (green) and far-future (red). Bottom and top of boxes indicate the 25th and 75th percentiles, respectively. Middle line is the ensemble median and whiskers extend to the lowest and highest ensemble member. See inset (a) for region masks (DAWR, 2016). (For interpretation of the references to colour in this figure legend, the reader is referred to the Web version of this article.)

decades in the country's southeast and southwest during certain months of the year (Dittus et al., 2014; Crimp et al., 2015). This has been attributed to decreasing soil moisture and subsequent increases in clear-sky conditions and larger nocturnal heat losses. That NARCliM does not exhibit this in regional means (Fig. 7b) or at the grid cell scale (Supplementary Fig. 15) could indicate that WRF does not capture frost dynamics adequately - as suggested in previous work (Andrys et al., 2017), that our seasonal (3 month) analyses are smoothing out trends at the monthly time scale or that increases in frost risk days will not continue into the future.

Increases in temperature and decreases in soil moisture are inherently related through sensible and latent heat partitioning (e.g. Donat et al., 2017). Calculation of the SPI reveals substantially less drought (in area and intensity) compared to the SPEI (cf. Supplementary Fig. 2 and Fig. 6), thus the additional drought estimated by the SPEI can be attributed to the impact of increasing temperatures on evapotranspiration. Mpelasoka et al. (2008) examined future drought projections also taking into consideration evapotranspiration and found similar patterns of change to those shown here (Fig. 6) though to a lesser extent, possibly due to their use of a more sophisticated soil moisture index and/or relatively coarse resolution global climate models (Mpelasoka et al., 2008). We also note the potential limitation of calculating evapotranspiration using the Hargreaves method, which assumes grass crop at all locations and which may bias our results toward dry values.

Madadgar et al. (2017) modelled the joint probability between observed crop yields and the October 6 month SPI from Australian rain-fed wheat growing regions. Combining their results with SPI calculated from NARCliM over all wheat growing regions (Fig. 7a inset)

Table 3
Published heat-health relationships and corresponding projections of health impacts based on the NARCliM ensemble median. Values in right three columns represent measures defined in the 'Units' column. [1]Where applicable, values in parentheses indicate increases in annual mortality (as a percentage or number of deaths) or increases in annual cases of Ross River Virus (as a percentage) based on the corresponding relationship. These estimates only consider the effect of future climates on the present day population (i.e. at the time of the corresponding study). See section 4.1 for details.[2] Williams et al. (2012a), study period: 1993–2009.[3]Guest et al. (1999), study period: 1979–1990.[4]Williams et al. (2012b), study period: 1994–2008.[5]Hu et al. (2008), study period: 1994–2004.[6]Bi et al. (2008), study period: 1986–1995.[7]Werner et al. (2012), study period: 1993–2009.

City[Ref]	Relationship	Units	Recent past	Near future[1]	Far future[1]
Adelaide[2]	Excess mortality increases during October–March on days where TX > 30 °C.	Days >30 °C	55 days	60 days	75 days
Adelaide[3]	Excess mortality of 0.6 during summer on days where TX > 30 °C.	Days >30 °C	36 days	41 days (3 extra deaths)	48 days (7.2 extra deaths)
Perth[4]	Excess mortality increases during November–April on days where TX > 35 °C.	Days >35 °C	20 days	25 days	40 days
Perth[3]	Excess mortality of 1 during summer on days where TX > 35 °C.	Days >35 °C	16 days	19 days (3 extra deaths)	30 days (14 extra deaths)
Sydney[5]	Increased excess mortality of 0.9% per°C in summer TX. 95% confidence interval (CI): 0.6–1.3%.	Summer TXm	29 °C	30 °C (0.9% extra deaths, CI: 0.6–1.3%)	31 °C (1.8% extra deaths, CI: 1.2–2.6%)
Sydney[3]	Excess mortality of 6.4 during summer on days where TX > 30 °C.	Days >30 °C	32 days	38 days (38.4 extra deaths)	44 days (76.8 extra deaths)
Brisbane[6]	Increased excess mortality of 7% per °C in monthly mean summer TX, for people 65 years and older.	Summer TXm	29.3 °C	29.8 °C (3.5% extra deaths)	31 °C (11.9% extra deaths)
Brisbane[3]	Excess mortality of 1.3 during summer on days where TX > 30 °C.	Days >30 °C	31 days	37 days (7.8 extra deaths)	56 days (32.5 extra deaths)
Melbourne[3]	Excess mortality of 2.9 during summer on days where TX > 30 °C.	Days >30 °C	20 days	24 days (11.6 extra deaths)	29 days (26.1 extra deaths)
Hobart[7]	Increased RRV cases of 23.2% per °C in monthly mean TX. 95% confidence interval (CI): 3–44%.	April TXm	16.5 °C	17.1 °C (14% more cases, CI: 1.8–26.4%)	18.4 °C (45% more cases, CI: 5.7–83.6%)

allows us to estimate the impact of projected soil-moisture conditions on Australian wheat yield. Relating the 6 month SPI value from all wheat growing regions for October from the NARCliM ensemble with the modelled probabilities from Madadgar et al. (2017), and using an annual historical wheat yield of 1602 kg/ha (based on 1980–2012 data, from Madadgar et al., 2017), there will be on average a 32% chance of exceeding the historical annual yield in the near future, and a 22% chance of exceeding it in the far future. Similar to our estimated health impacts, these values only consider the effects of climate change (and in fact only changes in precipitation), whereas significant future impacts would also come from reductions in frost damage (e.g. Nicholls, 1997), increased heat stress (e.g. Saini and Aspinall, 1982), increased CO_2 fertilization and direct anthropogenic interactions with the environment, such as deforestation or changes in water abstraction (Kiem et al., 2016). Advances in technology, improved farming practices, changes in farming locations and the breeding of better adapted wheat varieties (Zheng et al., 2012) could also affect future yields. The same statistical model based on the SPEI as opposed to the SPI would also likely show greater yield decreases.

Macadam et al. (2016) used output from the NARCliM ensemble to force a wheat crop model over the NSW wheat belt, in southeast Australia. In contrast to our estimate of future national wheat yields using the probabilities modelled by Madadgar et al. (2017), Macadam et al. (2016) modelled a mean increase in NSW wheat yield of approximately 800 kg/ha by the far future (also based on the 50 km bias-corrected NARCliM data). This conflicting result may be explained by the fact that the NSW wheat belt mostly lies outside the region of projected drought in the far future (Fig. 6). Furthermore, the physical crop model of Macadam et al. (2016) simulated a specific wheat variety (Ventura wheat) on a specific soil type (Brown clay) and considered CO_2 fertilization. Conversely, the statistical model developed by Madadgar et al. (2017) utilised wheat yield data over all soil types and wheat growing regions in the country and by definition did not consider CO_2 fertilization.

5. Conclusions

The NARCliM ensemble includes simulations over all of Australia at a 50 km spatial resolution for the recent past (1990–2009), near future (2020–2039) and far future (2060–2079), the latter two of which assume an intermediate emissions scenario (SRES A2). Consistent with previous climate projections for Australia, these simulations indicate increases in heat and drought related extremes throughout the 21st century. In the far future, day time temperature extremes are projected to increase by up to 3.5 °C depending on season and location. Moderate to severe drought conditions are also expected in the far future in the southwest and southeast during spring.

In addition to these results, we reveal new insights into potential changes in future climate extremes and assess their implications on the health and agricultural sectors. Heatwave frequency, number and duration will increase significantly in the near and far future, with greater increases in the north than south. All capital cities will experience at minimum a tripling of heatwave days each year by the far future compared to the recent past. For example, the number of heatwave days in Sydney each year will increase from 5.5 in the recent past to 23 in the far future. Implications for mortality are also severe, with projected future climates leading to increases in mortality due to high temperatures in all examined capital cities. The number of days at or above 30 °C in the major wheat growing regions will also increase substantially, particularly during spring when wheat is most vulnerable to temperature. Projected decreases in precipitation would decrease the likelihood of meeting historical production levels. Australian national wheat yields will have less than a one quarter chance of exceeding the annual historical average under projected far future precipitation change. Though this does not take into account the increases in heat stress, decreases in frost damage, increases in CO_2 fertilization and acclimatisation that would also occur under a future climate. Furthermore, while our analysis uses bias-corrected data, the correcting procedure assumes biases in the future are identical – in a distributional sense – to the biases of the recent past, which is unlikely true.

The NARCliM project is a publically available ensemble of regional climate model projections over the Australian continent, and at higher resolution over southeast Australia, capable of providing data at a spatial scale appropriate for regional planning. Combined with the ET-SCI indices it provides a suite of climate data for the 21st century that is easy to translate into sector impacts.

Acknowledgements

N.H. would like to acknowledge the work of Lukas Guske, Campbell Young, Nish Su and Roman Olson who have, at various times since 2015, contributed to data analysis in relation to this project. We would like to thank Shahrbanou Madadgar for providing the probability distributions used to calculate wheat yields under future climate scenarios. N.H. is supported by Australian Research Council grant CE110001028. J.K. is supported by an Australian Research Council Discovery Early Career Researcher Award (DE170100102). J.G. is supported by an Australian Postgraduate Award. We acknowledge support from the ARC Centre of Excellence for Climate Extremes (CE170100023). The NCAR Command Language (UCAR/NCAR/CISL/VETS 2016) and the Climate Data Operators (CDO) were used to create figures and process data.

Appendix A. Supplementary data

Supplementary data related to this article can be found at https://doi.org/10.1016/j.wace.2018.01.001.

References

Alexander, L., 2011. Climate science: extreme heat rooted in dry soils. Nat. Geosci. 4, 12–13.
Alexander, L.V., Arblaster, J.M., 2009. Assessing trends in observed and modelled climate extremes over Australia in relation to future projections. Int. J. Climatol. 29, 417–435. https://doi.org/10.1002/joc.1730.
Alexander, L.V., Arblaster, J.M., 2017. Historical and projected trends in temperature and precipitation extremes in Australia in observations and CMIP5. Weather Clim Extrem 15, 34–56. https://doi.org/10.1016/j.wace.2017.02.001.
Alexander L V, Nakaegawa T, Guelai FZ El, et al Development of climate indices for sector-specific applications.
Andrys, J., Kala, J., Lyons, T.J., 2017. Regional climate projections of mean and extreme climate for the southwest of Western Australia (1970–1999 compared to 2030–2059). Clim Dyn 48, 1723–1747. https://doi.org/10.1007/s00382-016-3169-5.
Argüeso, D., Di Luca, A., Evans, J., et al., 2015. Heatwaves Affecting NSW and the ACT: Recent Trends, Future Projections and Associated Impacts on Human Health. NARCliM Technical Note 5, Sydney, N.S.W.
Asseng, S., Foster, I.A.N., Turner, N.C., 2011. The impact of temperature variability on wheat yields. Global Change Biol. 17, 997–1012. https://doi.org/10.1111/j.1365-2486.2010.02262.x.
Bao, J., Sherwood, S.C., Alexander, L.V., Evans, J.P., 2017. Future increases in extreme precipitation exceed observed scaling rates. Nat. Clim. Change. https://doi.org/10.1038/nclimate3201.
Bi, P., Parton, K.A., Wang, J., Donald, K., 2008. Temperature and direct effects on population health in Brisbane, 1986-1995. J. Environ. Health 70, 48–53.
Bi, P., Williams, S., Loughnan, M., et al., 2011. The effects of extreme heat on human mortality and morbidity in Australia: implications for public health. Asia Pac. J. Publ. Health 23, 27S–36S. https://doi.org/10.1177/1010539510391644.
Clarke, H., Pitman, A.J., Kala, J., et al., 2016. An investigation of future fuel load and fire weather in Australia. Clim Change 139, 591–605. https://doi.org/10.1007/s10584-016-1808-9.
Coates, L., Haynes, K., O'Brien, J., et al., 2014. Exploring 167 years of vulnerability: an examination of extreme heat events in Australia 1844–2010. Environ. Sci. Pol. 42, 33–44. https://doi.org/10.1016/j.envsci.2014.05.003.
Cowan, T., Purich, A., Perkins, S., et al., 2014. More frequent, longer, and hotter heat waves for Australia in the twenty-first century. J. Clim. 27, 5851–5871. https://doi.org/10.1175/JCLI-D-14-00092.1.
Crimp, S., Bakar, K.S., Kokic, P., et al., 2015. Bayesian space–time model to analyse frost risk for agriculture in Southeast Australia. Int. J. Climatol. 35, 2092–2108. https://doi.org/10.1002/joc.4109.
Crimp, S.J., Gobbett, D., Kokic, P., et al., 2016. Recent seasonal and long-term changes in southern Australian frost occurrence. Clim Change 139, 115–128. https://doi.org/10.1007/s10584-016-1763-5.
DAWR, 2016. Catchment scale land use of Australia - update may 2016. http://data.gov.au/dataset/e981fa71-2ca8-4eea-a40e-e750a02f66d7.
Dittus, A.J., Karoly, D.J., Lewis, S.C., Alexander, L.V., 2014. An investigation of some unexpected frost day increases in southern Australia. Aust Meteorol Ocean J 64, 261–271.
Donat, M.G., Pitman, A.J., Seneviratne, S.I., 2017. Regional warming of hot extremes accelerated by surface energy fluxes. Geophys. Res. Lett. 44, 7011–7019. https://doi.org/10.1002/2017GL073733.
Ehret, U., Zehe, E., Wulfmeyer, V., et al., 2012. HESS Opinions "Should we apply bias correction to global and regional climate model data?". Hydrol. Earth Syst. Sci. 16, 3391–3404. https://doi.org/10.5194/hess-16-3391-2012.
Ekström, M., Grose, M.R., Whetton, P.H., 2015. An appraisal of downscaling methods used in climate change research. Wiley Interdiscip Rev Clim Chang 6, 301–319. https://doi.org/10.1002/wcc.339.
Evans, J., Argüeso, D., Olson, R., Di Luca, A., 2014a. NARCliM Extreme Precipitation Indices Report. Australia, Sydney.
Evans, J.P., Argüeso, D., 2014. Guidance on the Use of Bias Corrected Data. Sydney, Australia.
Evans, J.P., Argueso, D., Olson, R., Di Luca, A., 2016. Bias-corrected regional climate projections of extreme rainfall in south-east Australia. Theor. Appl. Climatol. https://doi.org/10.1007/s00704-016-1949-9.
Evans, J.P., Ji, F., Lee, C., et al., 2014b. Design of a regional climate modelling projection ensemble experiment – NARCliM. Geosci. Model Dev. (GMD) 7, 621–629. https://doi.org/10.5194/gmd-7-621-2014.
Firth, R., Kala, J., Lyons, T.J., Andrys, J., 2017. An analysis of regional climate simulations for western Australia's wine regions—model evaluation and future climate projections. J Appl Meteorol Climatol 56, 2113–2138. https://doi.org/10.1175/JAMC-D-16-0333.1.
Fita, L., Evans, J.P., Argüeso, D., et al., 2016. Evaluation of the regional climate response in Australia to large-scale climate modes in the historical NARCliM simulations. Clim Dyn 1–15. https://doi.org/10.1007/s00382-016-3484-x.
Gosling, S.N., Hondula, D.M., Bunker, A., et al., 2017. Adaptation to climate change: a comparative analysis of modeling methods for heat-related mortality. Environ. Health Perspect. 87008, 1.
Gross, M.H., Alexander, L.V., Macadam, I., et al., 2017. The representation of health-relevant heatwave characteristics in a regional climate model ensemble for New South Wales and the australian capital territory, Australia. Int. J. Climatol. 37, 1195–1210. https://doi.org/10.1002/joc.4769.
Guest, C.S., Willson, K., Woodward, A.J., et al., 1999. Climate and mortality in Australia: retrospective study, 1979-1990, and predicted impacts in five major cities in 2030. Clim. Res. 13, 1–15.
Hanna, E.G., Kjellstrom, T., Bennett, C., Dear, K., 2010. Climate change and rising heat: population health implications for working people in Australia. Asia Pac. J. Publ. Health 23, 14S–26S. https://doi.org/10.1177/1010539510391457.
Hansen, A., Bi, P., Nitschke, M., et al., 2008a. The effect of heat waves on mental health in a temperate australian city. Environ. Health Perspect. 116, 1369–1375. https://doi.org/10.1289/ehp.11339.
Hansen, A.L., Bi, P., Ryan, P., et al., 2008b. The effect of heat waves on hospital admissions for renal disease in a temperate city of Australia. Int. J. Epidemiol. 37, 1359–1365.
Herold, N., Kala, J., Alexander, L.V., 2016. The influence of soil moisture deficits on Australian heatwaves. Environ. Res. Lett. 11, 64003.
Hu, W., Mengersen, K., McMichael, A., Tong, S., 2008. Temperature, air pollution and total mortality during summers in Sydney, 1994–2004. Int. J. Biometeorol. 52, 689–696. https://doi.org/10.1007/s00484-008-0161-8.
Huang, C., Barnett, A.G., Wang, X., et al., 2011. Projecting future heat-related mortality under climate change scenarios: a systematic review. Environ. Health Perspect. 119, 1681–1690. https://doi.org/10.1289/ehp.1103456.
Hughes, L., Steffen, W., 2014. Heatwaves: Hotter, Longer, More Often.
Hughes, L., Steffen, W., Rice, M., Pearce, A., 2015. Feeding a Hungry Nation: Climate Change, Food and Farming in Australia.
IPCC, 2012. Summary for policymakers. Manag. Risks extrem. Events disasters to adv. Clim. Chang. Adapt. A Spec. Rep. Work. Groups I II Intergov. Panel Clim. Chang 3–21.
IPCC, 2013. Climate Change 2013: the Physical Science Basis. Contribution of Working Group I to the Fifth Assessment Report of the Intergovernmental Panel on Climate Change [Stocker, T.F., D. Qin, G.-K. Plattner, M. Tignor, S.K. Allen, J. Boschung, A. Nauels, Y. Xia., Cambridge, United Kingdom and New York, NY, USA).
Jegasothy, E., McGuire, R., Nairn, J., et al., 2017. Extreme climatic conditions and health service utilisation across rural and metropolitan New South Wales. Int. J. Biometeorol. 61, 1359–1370. https://doi.org/10.1007/s00484-017-1313-5.
Jones, D.A., Wang, W., Fawcett, R., 2009. High-quality spatial climate data-sets for Australia. Aust Meteorol Oceanogr J 58, 233.
Kala, J., Lyons, T.J., Foster, I.J., Nair, U.S., 2009. Validation of a simple steady-state forecast of minimum nocturnal temperatures. J Appl Meteorol Climatol 48, 624–633. https://doi.org/10.1175/2008JAMC1956.1.
Karl, T.R., Knight, R.W., 1997. The 1995 chicago heat wave: how likely is a recurrence? Bull. Am. Meteorol. Soc. 78, 1107–1119. https://doi.org/10.1175/1520-0477(1997)078<1107:TCHWHL>2.0.CO;2.
Kiem, A.S., Johnson, F., Westra, S., et al., 2016. Natural hazards in Australia: droughts. Clim Change 139, 37–54. https://doi.org/10.1007/s10584-016-1798-7.
Kirono, D.G.C., Kent, D.M., Hennessy, K.J., Mpelasoka, F., 2011. Characteristics of Australian droughts under enhanced greenhouse conditions: results from 14 global climate models. J. Arid Environ. 75, 566–575. https://doi.org/10.1016/j.jaridenv.2010.12.012.
Langlois, N., Herbst, J., Mason, K., et al., 2013. Using the Excess Heat Factor (EHF) to predict the risk of heat related deaths. J Forensic Leg Med 20, 408–411. https://doi.org/10.1016/j.jflm.2012.12.005.
Loughnan, M., Nicholls, N., Tapper, N., 2010a. Mortality–temperature thresholds for ten major population centres in rural Victoria, Australia. Health Place 16, 1287–1290. https://doi.org/10.1016/j.healthplace.2010.08.008.
Loughnan, M.E., Nicholls, N., Tapper, N.J., 2010b. The effects of summer temperature, age and socioeconomic circumstance on Acute Myocardial Infarction admissions in Melbourne, Australia. Int. J. Health Geogr. 9, 41. https://doi.org/10.1186/1476-072X-9-41.
Macadam, I., Argüeso, D., Evans, J.P., et al., 2016. The effect of bias correction and climate model resolution on wheat simulations forced with a regional climate model ensemble. Int. J. Climatol. 36, 4577–4591. https://doi.org/10.1002/joc.4653.
Madadgar, S., AghaKouchak, A., Farahmand, A., Davis, S.J., 2017. Probabilistic estimates of drought impacts on agricultural production. Geophys. Res. Lett. https://doi.org/10.1002/2017GL073606 n/a-n/a.

Marcellos, H., Single, W.V., 1975. Temperatures in wheat during radiation frost. Aust. J. Exp. Agric. 15, 818–822.
McKee, T.B., Doesken, N.J., Kleist, J., 1993. The Relationship of Drought Frequency and Duration to Time Scales. in: Proceedings of the 8th Conference on Applied Climatology. American Meteorological Society Boston, MA, USA, pp. 179–183.
Meehl, G.A., Covey, C., Taylor, K.E., et al., 2007. THE WCRP CMIP3 multimodel dataset: a new era in climate change research. Bull. Am. Meteorol. Soc. 88, 1383–1394. https://doi.org/10.1175/BAMS-88-9-1383.
Monteith, J., Unsworth, M., 2013. Principles of Environmental Physics: Plants, Animals, and the Atmosphere. Academic Press.
Mpelasoka, F., Hennessy, K., Jones, R., Bates, B., 2008. Comparison of suitable drought indices for climate change impacts assessment over Australia towards resource management. Int. J. Climatol. 28, 1283–1292. https://doi.org/10.1002/joc.1649.
Nairn, J.R., Fawcett, R.G., 2013. Defining Heatwaves: Heatwave Defined as a Heat-impact Event Servicing All Community and Business Sectors in Australia. Centre for Australian Weather and Climate Research.
Naish, S., Hu, W., Nicholls, N., et al., 2009. Socio-environmental predictors of Barmah forest virus transmission in coastal areas, Queensland, Australia. Trop. Med. Int. Health 14, 247–256.
Nicholls, N., 1997. Increased Australian wheat yield due to recent climate trends. Nature 387, 484.
OEH, 2017. NSW climate data portal. In: off. Environ. Herit. https://climatedata.environment.nsw.gov.au/. (Accessed 27 September 2017).
Olson, R., JP, E., DL, A., Argüeso, D., 2016. The NARCliM project: model agreement and significance of climate projections. Clim. Res. 69, 209–227.
Oppermann, E., Brearley, M., Law, L., et al., 2017. Heat, health, and humidity in Australia's monsoon tropics: a critical review of the problematization of "heat" in a changing climate. Wiley Interdiscip Rev Clim Chang 8. https://doi.org/10.1002/wcc.468 e468–n/a.
Pearce, J.L., Hyer, M., Hyndman, R.J., et al., 2016. Exploring the influence of short-term temperature patterns on temperature-related mortality: a case-study of Melbourne, Australia. Environ. Health 15, 107. https://doi.org/10.1186/s12940-016-0193-1.
Perkins, S.E., Alexander, L.V., 2013. On the measurement of heat waves. J. Clim. 26, 4500–4517. https://doi.org/10.1175/JCLI-D-12-00383.1.
Perkins, S.E., Pitman, A.J., 2009. Do weak AR4 models bias projections of future climate changes over Australia? Clim Change 93, 527–558. https://doi.org/10.1007/s10584-008-9502-1.
Peters, G.P., Andrew, R.M., Boden, T., et al., 2013. The challenge to keep global warming below 2 [deg]C. Nat. Clim. Change 3, 4–6.
PwC, 2011. Protecting Human Health and Safety during Severe and Extreme Heat Events: a National Framework.
Saini, H.S., Aspinall, D., 1982. Abnormal sporogenesis in wheat (Triticum aestivum L.) induced by short periods of high temperature. Ann. Bot. 49, 835–846.
Scalley, B.D., Spicer, T., Jian, L., et al., 2015. Responding to heatwave intensity: excess Heat Factor is a superior predictor of health service utilisation and a trigger for heatwave plans. Aust. N. Z. J. Publ. Health 39, 582–587. https://doi.org/10.1111/1753-6405.12421.
Shamarock, W., Klemp, J.B., Dudhia, J., et al., 2008. A Description of the Advanced Research WRF. NCAR Technical Note TN–475+ STR, Version 3. .
Sherwood, S.C., Huber, M., 2010. An adaptability limit to climate change due to heat stress. Proc. Natl. Acad. Sci. Unit. States Am. 107, 9552–9555.
Sillmann, J., Kharin, V.V., Zwiers, F.W., et al., 2013. Climate extremes indices in the CMIP5 multimodel ensemble: Part 2. Future climate projections. J. Geophys. Res. Atmos. 118, 2473–2493. https://doi.org/10.1002/jgrd.50188.
Taylor, K.E., Stouffer, R.J., Meehl, G.A., 2011. An overview of CMIP5 and the experiment design. Bull. Am. Meteorol. Soc. 93, 485–498. https://doi.org/10.1175/BAMS-D-11-00094.1.
Teague, B., McLeod, R., Pascoe, S., 2010. Victorian Bushfires Royal Commission. Final report, 2009.
Tebaldi, C., Arblaster, J.M., Knutti, R., 2011. Mapping model agreement on future climate projections. Geophys. Res. Lett. 38 https://doi.org/10.1029/2011GL049863 n/a–n/a.
Tong, S., Wang, X.Y., Barnett, A.G., 2010. Assessment of heat-related health impacts in Brisbane, Australia: comparison of different heatwave definitions. PLoS One 5, e12155.
Turner, L.R., Connell, D., Tong, S., 2013. The effect of heat waves on ambulance attendances in Brisbane, Australia. Prehospital Disaster Med. 28, 482–487, 10.1017/S1049023X13008789.
UCAR/NCAR/CISL/VETS, 2016. The NCAR Command Language ([Software]), Version 6.3. .
van Dijk, A.I.J.M., Beck, H.E., Crosbie, R.S., et al., 2013. The Millennium Drought in southeast Australia (2001–2009): natural and human causes and implications for water resources, ecosystems, economy, and society. Water Resour. Res. 49, 1040–1057. https://doi.org/10.1002/wrcr.20123.
VGDHS, 2009. Heatwave in Victoria: an Assessment of Health Impacts. Victorian Government Department of Human Services, Melbourne, Melbourne. January 2009.
Vicente-Serrano, S.M., Beguería, S., López-Moreno, J.I., 2010. A multiscalar drought index sensitive to global warming: the standardized precipitation evapotranspiration index. J. Clim. 23, 1696–1718. https://doi.org/10.1175/2009JCLI2909.1.
Wang, B., Liu, D.L., Macadam, I., et al., 2016. Multi-model ensemble projections of future extreme temperature change using a statistical downscaling method in south eastern Australia. Clim Change 138, 85–98. https://doi.org/10.1007/s10584-016-1726-x.
Werner, A., Goater, S., Carver, S., et al., 2012. Environmental drivers of Ross River virus in southeastern Tasmania, Australia: towards strengthening public health interventions. Epidemiol. Infect. 140, 359–371. https://doi.org/10.1017/S0950268811000446.
Westra, S., White, C.J., Kiem, A.S., 2016. Introduction to the special issue: historical and projected climatic changes to Australian natural hazards. Clim Change 1–19. https://doi.org/10.1007/s10584-016-1826-7.
Williams, S., Nitschke, M., Sullivan, T., et al., 2012a. Heat and health in Adelaide, South Australia: assessment of heat thresholds and temperature relationships. Sci. Total Environ. 414, 126–133. https://doi.org/10.1016/j.scitotenv.2011.11.038.
Williams, S., Nitschke, M., Weinstein, P., et al., 2012b. The impact of summer temperatures and heatwaves on mortality and morbidity in Perth, Australia 1994–2008. Environ. Int. 40, 33–38. https://doi.org/10.1016/j.envint.2011.11.011.
WMO, 2012. Standardized Precipitation Index User Guide. 7 bis, avenue de la Paix – P.O. Box 2300 – CH 1211 Geneva 2–Switzerland.
Zander, K.K., Botzen, W.J.W., Oppermann, E., et al., 2015. Heat stress causes substantial labour productivity loss in Australia. Nat. Clim. Change 5, 647–651.
Zheng, B., Chenu, K., Fernanda Dreccer, M., Chapman, S.C., 2012. Breeding for the future: what are the potential impacts of future frost and heat events on sowing and flowering time requirements for Australian bread wheat (Triticum aestivum) varieties? Global Change Biol. 18, 2899–2914. https://doi.org/10.1111/j.1365-2486.2012.02724.x.